Research Article | Vol. 29, No. 8 / 12 April 2021 / Optics Express 12252
Optics EXPRESS

Compensation of SOA-induced nonlinear phase distortions by optical phase conjugation

ANEESH SOBHANAN,[1] MARK PELUSI,[2,3] TAKASHI INOUE,[2] DEEPA VENKITESH,[1,4] AND SHU NAMIKI[2]

[1]Department of Electrical Engineering, Indian Institute of Technology Madras, Chennai 600 036, India
[2]National Institute of Advanced Industrial Science and Technology, Tsukuba 305-8568, Japan
[3]m.pelusi@aist.go.jp
[4]deepa@ee.iitm.ac.in

Abstract: To answer the question: "Is optical phase conjugation (OPC) capable of compensating nonlinear distortions caused by not only Kerr effect of optical fibre, but also the carrier dynamics of semiconductor optical amplifiers (SOAs)?", we investigate the effectiveness of OPC-based nonlinear compensation for SOAs amplifying a few-channel WDM signal modulated with m-QAM. We use a pair of SOAs with an OPC stage sandwiched between the two so that the combination works as a low-distortion amplifier. Symbol-period longer than the gain recovery time is chosen in our experiments to avoid bit-pattern effects introduced by the SOA. We amplify a 12Gbaud, 16QAM modulated three-channel WDM signal with this technique in the back-to-back configuration which remarkably outperforms a single SOA in the nonlinear regime of operation with an average Q^2 improvement better than 4 dB for an output power of 4 dBm. We further demonstrate the practical advantage of the low distortion higher output power capability of the SOA shown in the back-to-back result by carrying out a transmission of the amplified signal through a 160-km fibre, where relatively high launch power is desirable. We also study the case of 64QAM signals and show that approximately a 3 dB Q^2 factor improvement can be obtained over single SOA, while without nonlinear phase distortion compensation, the demodulation is nearly impracticable.

1. Introduction

Increased demand for capacity in fiber optic communication systems has led to investigations in expanding the operating wavelengths of optical amplifiers beyond the C and the L-bands. In this context, semiconductor optical amplifiers have attracted renewed interest in the recent past due to the feasibility of ultra-wideband amplification [1]. It is well-known that SOA-based amplification induces amplitude distortions in the signal because of bit pattern effects, originating due to the slow gain recovery time of the SOA compared to the symbol duration. The pattern effects are typically avoided by operating SOAs in a linear, small-signal regime. However, there are many situations- in particular involving higher capacity optical signals such as WDM, where SOAs do not typically operate in a linear regime. In such cases, one has to use symbol rates smaller than the inverse of the gain recovery time [2], use holding beam [3] or thoroughly change the design of SOAs [4,5].

Even while using the SOAs whose gain recovery time is sufficiently shorter than the unit interval of the signal and thus successfully avoiding the amplitude distortions, the optical signals will still be subject to nonlinear phase distortions, originating from the fast carrier density change caused by rapidly changing optical intensity associated with the intra- and inter-channel random beats of the broadband optical signals. Signals modulated with advanced modulation formats are especially susceptible to phase distortions. An extensive study of phase distortions due to gain fluctuations in the nonlinear operating regime of SOAs is carried out in [6]. Mitigation of nonlinear distortions in SOA is demonstrated in the past using all-optical methods [7–11] and

#416955 https://doi.org/10.1364/OE.416955
Journal © 2021 Received 9 Dec 2020; revised 15 Feb 2021; accepted 16 Feb 2021; published 6 Apr 2021

Optics EXPRESS

through digital signal processing (DSP) [12–15]. The DSP techniques need consideration of computational complexity. Optimized operations of ultra-wideband SOAs for massive WDM channel counts are reported recently [1,16]. Spreading the power of the optical field with a large number of independent channels greatly reduces the power fluctuations at the input, which in turn decreases the nonlinear distortions induced by the SOA [1]. However, for a few WDM channels, the power fluctuations can be large, resulting in a significant phase distortion [1,16]. Thus, the utility of SOAs for amplification becomes questionable when only few WDM channels are operated, which is a plausible scenario in future short-distance/access and data center networks. Hence it is interesting to scrutinize a method for compensating the phase distortions suffered by fewer channel WDM signals with typical off-the-shelf SOAs.

In this work, we investigate the efficacy of optical phase conjugation (OPC) to reduce the nonlinear phase distortions from SOAs. We use an OPC stage sandwiched between a pair of commercial “nonlinear" SOAs (with a gain recovery time of <25 ps as per Kamelian SOA product specification sheet). The symbol-rate used in this study is 12 Gbaud, with a corresponding symbol period of 83 ps, which is slower than the gain recovery time. Thus, bit pattern effects are well suppressed in our study. In this SOA-OPC-SOA configuration, the combination of OPC and the second SOA, or OPC-SOA, serves to null the distortion from the first SOA. In other words, OPC-SOA is considered as a nonlinear compensator (NLC) and hence this configuration is referred to as SOA-NLC. Mid-span OPC method is well-known for compensating nonlinear distortion in long-distance optical fiber links arising from the Kerr effect [17–19]. Modulation format agnostic optical phase conjugation has been demonstrated in the past using different nonlinear media such as highly nonlinear fibers (HNLFs) [20], periodically poled lithium niobate waveguides [21], silicon waveguides [22], and SOAs [23,24]. Here, we investigate the efficacy of OPC to compensate for the phase distortions due to an SOA. We generate the phase conjugate with a state-of-the-art HNLF, for the proof of principle experiment. We focus on the nonlinear phase distortions due to the dynamic changes in the gain of SOAs, where the bit-pattern effect is negligibly small.

Preliminary results of the back-to-back operation of the SOA-NLC scheme for a three-channel WDM system in 16QAM modulation was presented in our previous report [25], where we compared its performance to that with single SOA at a specific SOA input power. The advantage of the scheme in a long link fiber transmission was also briefly discussed. In this paper, we first review the operating principle and identify the conditions under which the SOA-NLC scheme is expected to be beneficial, followed by a discussion of the details of the experimental setup. We specifically identify the regime of operation where the SOA-NLC scheme outperforms the single SOA. Further, the amplified signal from the SOA-NLC is transmitted through a 160 km fiber. Comparing its performance with that of an amplified signal from a single SOA, it is shown that the SOA-NLC outperforms the single SOA even in its linear operating regime. The benefit of the scheme is expected to be more pronounced in modulations with higher cardinality because of the corresponding decreased tolerable phase margin and hence we demonstrate this for 64QAM modulated WDM channels. These results along with the implementation of OPC in SOAs [25], can be a promising technique for the 1.3 μm amplifier solution in future.

2. Operating principle

The block diagram explaining the working principle of the OPC-based nonlinearity compensation scheme is shown in Fig. 1. Representative constellation diagrams corresponding to 16QAM modulation, expected at the output of each stage are also shown. We convey the concept of this scheme using equations of a basic model, without describing the detailed theoretical models of SOA and its dynamics which can be found in [26]. The optical signal from the transmitter is the input to the first SOA and its output is expected to have gain, but with a distorted constellation as shown in the Fig. 1(a). The output field of the first SOA $E_i'(t)$, assuming the envelope of the input

Optics EXPRESS

is not distorted due to pattern effect, is represented as [1],

$$E_i'(t) = E_i(t)\exp\left[\frac{1}{2}(1 - j\alpha_{H1})h_1(t)\right], \tag{1}$$

where, $E_i(t)$ represents the electric field of the modulated input signal, α_{H1} is Henry's linewidth enhancement factor, $h_1(t)$ is the integrated gain coefficient and $G_1 = \exp(h_1(t))$ the power gain of the first SOA. The above equation also ignores the wavelength dependence [27] and the polarization dependence [28] of the integrated gain coefficient $h_1(t)$. For the SOAs used in the experiment, we have independently verified that the difference in gain between the three-wavelength channels used (with a uniform separation of 0.4 nm) is less than 0.5 dB and we have also used data modulated in a single polarization, which justify these assumptions. The influences of spectral hole burning, carrier heating and two-photon absorption, which can be found in [29], are also not considered in the presented equations as those ultra-fast processes have a negligible effect in the symbol duration and the frequency separation of the WDM channels of our interest.

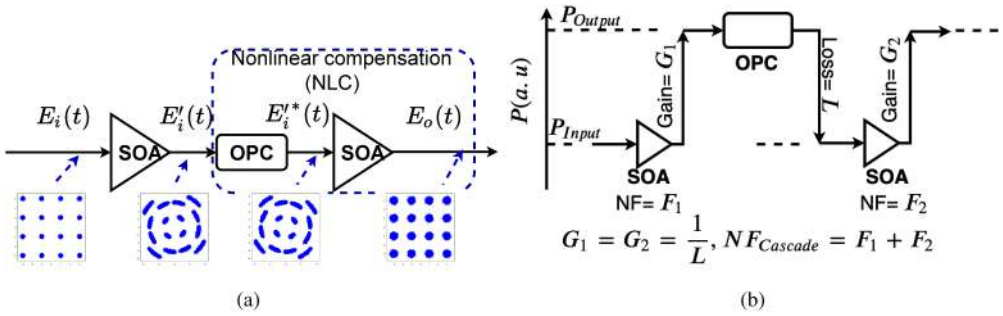

Fig. 1. (a) Schematic of SOA-NLC with OPC sandwiched between two SOAs (b) power distribution map (in the ideal case) indicating the power levels and noise figure at the output of the SOA-NLC scheme.

Outside the small-signal regime, any time-dependent change in the amplitude of input signal results in a corresponding change in the gain, which in turn results in nonlinear phase modulation. As $h_1(t)$ acts as homogeneously broadened gain shared by WDM channels, both self and cross-phase modulation are present in a WDM system. To compensate the distortions due to such nonlinear phase modulation, we use an optical phase conjugation stage, followed by a second SOA. The electric field $E_i'^*(t)$ at the OPC output, under ideal conditions, is written as:

$$E_i'^*(t) = E_i^*(t)\exp\left[\frac{1}{2}\left(1 + j\alpha_{H1}\right)h_1(t) - \alpha_L\right], \tag{2}$$

where $E_i^*(t)$ denotes the conjugate of the electric field of the input signal, α_L is the loss coefficient such that $\exp(-2\alpha_L)$ represents the loss at the OPC stage, depending on its conversion efficiency. Now the output field of the second SOA, $E_o(t)$, is given by:

$$E_o(t) = E_i'^*(t)\exp\left[\frac{1}{2}\left(1 - j\alpha_{H2}\right)h_2(t)\right], \tag{3}$$

where α_{H2} is Henry's linewidth enhancement factor and $h_2(t)$ is the integrated gain coefficient of the second SOA. For a very simplistic design approach to achieve nonlinear distortion compensation using two SOAs, we assume that both the SOAs have similar linewidth enhancement factor. For

Optics EXPRESS

a given input power and drive current we also assume $h_1(t) = h_2(t)$. Thus the SOA-NLC output can be written as:

$$E_o(t) = E_i^*(t) \exp\left[h_1(t) - \alpha_L\right], \tag{4}$$

If the loss in the OPC stage is adjusted by ensuring $G_1 = \exp(-2\alpha_L)$, the output of SOA-NLC combination can be expressed as:

$$E_o(t) = E_i^*(t) \exp\left[\frac{1}{2}h_1(t)\right]. \tag{5}$$

Thus the SOA-NLC scheme offers the same power gain $G_2 = G_1 = \exp(h_1(t))$ as the single-SOA scheme but without the phase distortion. It is noted that amplified spontaneous emission (ASE) noise is added by both the SOAs and is not explicitly included in the equations discussed above.

We assume that the nonlinear distortions that are expected to be compensated for, are dominated by self- and cross-phase modulation (XPM) and the bit-pattern effect is ignored. In the presence of the bit pattern effect, the envelope of the output of the first SOA could be changed with respect to the input. The OPC stage reverses only the phase of the input, while the envelope remains unchanged. The envelope will be further distorted after the second SOA regardless of the OPC stage, invalidating the requirement that $h_1(t)$ should be equal to $h_2(t)$. In other words, such envelope changes do not allow the second SOA to induce similar instantaneous nonlinear distortions as that of the first SOA, which may hamper the effectiveness of the OPC for phase compensation. In this study, we adopt a strategy to focus on the cases where $h_1(t)$ and $h_2(t)$ have as similar temporal shape as possible by means of suppressing bit-pattern effects.

The scheme requires the two SOAs to operate at the same gain, and hence the loss in the OPC stage must not be larger than the gain of either of the SOAs. For experiments investigating different input power levels and gain of first SOA, the loss of the OPC stage should be manually adjusted to maintain the requisite gain-loss condition. Since our experiments use two discrete SOAs, we carried out a detailed characterization to identify the operating point, which satisfies the symmetric performances in terms of wavelength, gain and nonlinearity. The ideal power excursion across the different elements are shown in Fig. 1(b). As shown in the figure, considering OPC only as a loss element ($L = \exp(-2\alpha_L)$), since the gain compensates for the loss in the OPC stage ($G = G_1 = G_2 = 1/L$), the total noise figure (NF) would be approximately $F_1 + F_2 - \frac{1}{G}$. When the gain G is large, it is approximately $F_1 + F_2$, where F_1 and F_2 are the noise figures of the two SOAs respectively. This approach is expected to provide performance improvement (in terms of BER and Q^2) over the single SOA despite the additional ASE noise from the second SOA because of the compensation of the phase distortions.

3. Experimental setup

Schematic of the experimental setup for three-channel WDM system in a back-to-back configuration with SOA/SOA-NLC is shown in Fig. 2 where the performance of an SOA amplifier with and without optical phase conjugate based compensator is studied. In the transmitter, three CW lasers (external cavity laser of narrow linewidth < 100kHz) at frequencies (f_s) 192.65 THz ± 50 GHz are modulated with a single polarization IQ modulator at 12 Gbaud, with 16QAM and 64QAM symbols generated by a two-channel arbitrary waveform generator (12 GS/s) with a PRBS $2^{15} - 1$ pattern, thus generating 3× 48 and 3×72 Gbps WDM signal respectively. Data in each of these WDM channels are decorrelated by propagating it through 80 km of single mode fiber, which provides a decorrelation of > 540 ps between the channels. The net input power to the decorrelating 80 km fiber is maintained at 2 dBm to ensure that the signal propagation through the fiber is approximately linear. This decorrelated 3×12 Gbaud 16QAM/64QAM WDM-signal is amplified by the first SOA stage (saturation power, P_{sat}= 10 dBm).

Optics EXPRESS

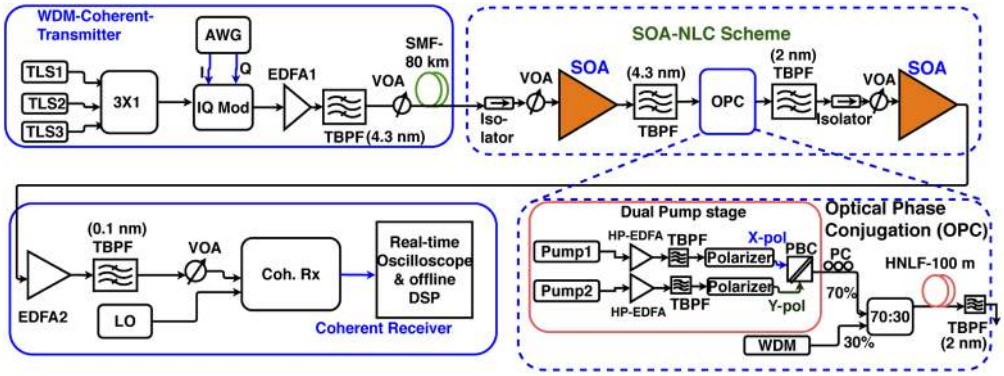

Fig. 2. Schematic of the experimental setup showing the nonlinear distortion compensation using phase conjugation. The block diagram of the OPC is also shown.

The amplified, but the phase distorted output from the first SOA is fed as the input to the OPC stage. For this proof-of-principle study, we choose an OPC using HNLF with minimal distortions and largest bandwidth and conversion efficiency, to ensure that the observed results are only caused by the nonlinear distortions and any observed OSNR degradation is due to the SOAs and not due to OPC. The impact of a simpler OPC implementation with a single pump instead of two pumps and reduced conversion efficiency with lower pump power, on the SOA nonlinear distortion compensation is not investigated in this paper. Such OPC with lower conversion efficiency performs without much penalty for signals with smaller input OSNR values [30]. Feasibility of OPC using SOA with low pump power (1 mW) has been demonstrated [23] and such implementation could make the pump EDFA unnecessary. BPF could also become redundant if pump EDFA is avoided. Notably, a requirement for an EDFA for either the input signal or output conjugate in the OPC set-up is made redundant by ensuring (a) the total loss in the OPC stage is well below the SOA gain over the input power range considered in the experiment, and (b) the input signal power induces negligible distortion in the power range considered at the OPC stage such that the conjugate performance penalty is < 0.5 dB. OPC setup without polarization controllers (PC) could be possible by using polarization maintaining components in polarization diversity configurations [31–33]. However, low-distortion OPC with SOA for such low OSNR, amplified and distorted signal from SOA is unproven and likely has challenges. This work focuses particularly on the potential of OPC for compensating the nonlinear phase distortion introduced by the SOA.

Light from two pump lasers (frequencies $f_{P1} = 191.7$ THz, $f_{P2} = 194$ THz) is amplified using independent high-power amplifiers, filtered and combined using polarization beam combiner (PBC) to ensure that the pumps entering the HNLF are orthogonally polarized to generate polarization-insensitive OPC [19]. Irrespective of the polarization states of the three channels at the input of the OPC stage the polarization diverse scheme ensures a polarization-insensitive conjugate generation. It is also ensured that the pump power launched into the 100 m long HNLF is 26 dBm, which is smaller than the Brillouin threshold of the fiber. 1% of the power is fed to the optical spectrum analyzer through 8×1 switch and tap-couplers from all the relevant stages for monitoring the gain values. The OSNR is measured after the pre-amplifier (EDFA2) in the receiver side on an OSA, with RBW of 0.2 nm, noise reference bandwidth of 0.1 nm and the offset wavelength of 0.8 nm from the center channel. The conjugate of the WDM signals with a conversion efficiency (the ratio of phase conjugate power at the output to the signal power at the input of the HNLF in the OPC stage) of -7 dB is generated at a frequency ($f_c = f_{P1} + f_{P2} - f_s$) 193.05 $\mp$ 50 GHz. This estimate, however, does not account for the different path loss differences

Optics EXPRESS

expected primarily from the uncalibrated tap couplers (assumed both as ideal 99:1). HNLF being a parametric nonlinear medium and since the noise transfer from the pumps is negligibly small, the OSNR degradation at the OPC stage is negligibly small. The operating points are chosen such that the SOA nonlinear distortions are symmetric with respect to gain and wavelength and the details of this characterization are explained in Appendix A. This characterization is specific to the choice of the SOAs used. The two devices could have well-matched properties if fabricated as a part of the same substrate and processed similarly and in that case, such detailed characterization may not be necessary.

The polarization-dependent loss of both the SOAs is less than 0.5 dB and hence the input state of polarization to each SOA is arbitrarily chosen. We use tunable band-pass filter (TBPF) of bandwidth 4.3 nm as an ASE filter for removing large out of band noise to the OPC stage. We use another TBPF of bandwidth 2 nm after the OPC stage to filter the conjugates, thereby ensuring that there is no signal leakage into the filtered band. Thus, it is to be noted that we use different filter bandwidths for SOA and SOA with OPC experiments. The use of different filter bandwidths is not expected to significantly change the results since the difference in noise power at the input of the two SOAs due to this change in filter bandwidth is not significant enough to change the SOA dynamics at these operating OSNRs. Furthermore, the receiver includes a 0.1 nm narrow bandwidth filter and hence, the ASE noise power at receiver could not be affected by this change in the filter bandwidths.

The output of the second SOA is fed to a polarization diverse-coherent receiver and a real-time oscilloscope (33 GHz and 80 GSa/s). The frequency of the local oscillator laser is adjusted close to that of the WDM signal that is demodulated. Further offline digital signal processing is used to calculate BER and Q^2 values of all the WDM channels. The method used to measure the Q^2-factor from the experimental data is explained in Appendix B. Using the $BER - Q$ and $OSNR - SNR$ relations in [34] and $BER - SNR$ relation for m-QAM signals in [35] (see Appendix C), we obtain the theoretical value of Q^2 as 12.3 dB for 16QAM signal at OSNR 16 dB and 13.2 dB for 64QAM at OSNR of 23 dB, at a symbol rate of 12 Gbaud. The lower OSNR values are chosen for theoretical calculation so that it emulates more precisely the noise sources of the distortion in a back-to-back system experiment. The experimental system penalty with respect to the theoretically expected value of Q^2 for a 12 Gbaud 16QAM signal is 2.6 dB and for 64QAM signal is around 4.4 dB. The OPC and the second SOA stage are bypassed for generating the results corresponding to a single SOA. We also compare the performance of a single SOA with that of an SOA with the NLC, when used as an amplifier with a long fiber span. For these experiments, a 160 km long fiber is connected *after* the SOA / SOA-NLC stage. We carried out all the experiments with the same input power at the receiver, which is ensured to be above its sensitivity limit.

4. Results and discussion

4.1. Back-to-back operation

We first discuss the results with a 16QAM WDM signal in the back-to-back configuration. Same input power P_{in} and driving current I_{drive} (150 mA) are maintained at both the SOAs. The input and output spectra at the OPC stage is shown in Fig. 3. The input OSNR to the OPC stage is low (<30 dB) that any additional OSNR degradation from the OPC stage itself (due influences such as low FWM conversion efficiency and limited extinction ratio of pump filters) has insignificant impact on overall OSNR at receiver [30]. The constellation plots for different stages of the experiments for the first WDM channel (192.60 THz, with phase conjugate at 193.10 THz) are also shown in Fig. 3. Input signal power is chosen to be -14.5 dBm, corresponding to an operating regime where the signal is expected to undergo nonlinear distortions, and the operating wavelengths are chosen as per the optimization discussed in Appendix A. The signal constellation is phase distorted after the SOA without NLC. The constellation which is laterally

Optics EXPRESS

inverted at the output of OPC clearly demonstrates a conjugated effect. After the NLC element following the first SOA, a constellation without nonlinear distortion is obtained. The gain (per channel) is found to be ≈ 18 dB both for the single SOA and for the SOA-NLC. The OSNR at the SOA-NLC output shows degradation of ∼ 3.2 dB compared to that from single SOA output as expected. The SOA-NLC output with OPC shows low-distortion despite the effective approximate double nonlinear distortion and noise from the pair of cascaded SOAs. This result establishes the effectiveness of the OPC in this scheme.

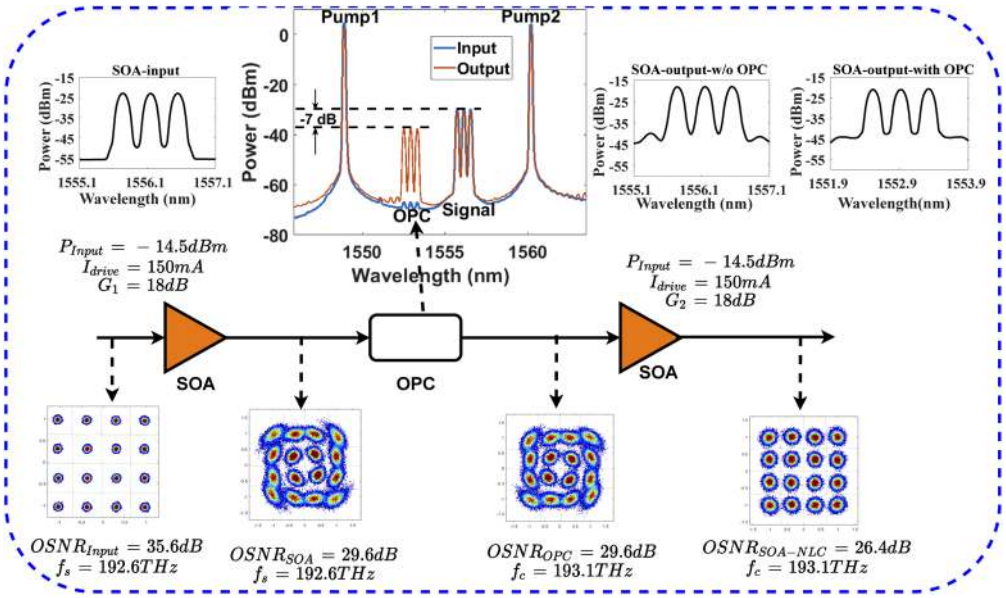

Fig. 3. Constellations at different stages (Ch1) ; P_{in}= -14.5 dBm and I_{drive}= 150 mA. The spectra at the input of the SOA and the output of the SOA with and without OPC are shown for understanding the changes in the spectra in the presence and absence of OPC stage. The input and output spectra of the OPC stage is also shown with conversion efficiency of -7 dB marked.

4.2. Influence of input power levels

It may be argued that the nonlinear distortions of the SOA can be minimized by operating in its linear regime, but this could limit the achievable power at the output of the SOA. To identify the range of power inputs where this OPC scheme is beneficial, we further vary the input power to the SOA from -24.5 dBm to -12.5 dBm to obtain the corresponding output power in the range of -5 dBm to +4 dBm.The performance is quantified by evaluating the Q^2 value for each WDM channel, for both single SOA and SOA-NLC. The Q^2 performance for all the three channels as a function of output power is shown in the left y-axis of Fig. 4. The plot also shows the OSNR measured at the receiver end as $OSNR_{out}$ on the right-side y-axis. The OSNR improves with the increase in output power for both SOA and SOA-NLC cases since the ASE power decreases with an increase in input power. The OSNR of the SOA-NLC output is smaller compared to that of the single SOA output in all the three channels because of the additional noise figure from the second SOA. The difference in OSNR also decreases with an increase in output power due to a decrease in the ASE power. We find poorer Q^2 performance at the low output power values (< 0 dB) with SOA-NLC compared to single SOA. The WDM signals undergo minimal nonlinear distortions at these low output power values and hence the output from the single SOA is expected to have good performance. The output from SOA-NLC, though distortion compensated, experiences larger

Optics EXPRESS

noise, and hence smaller Q^2 compared to that of single SOA. With the increase in input power, the output of the single SOA degrades in performance due to a large phase distortion while that of the SOA-NLC improves. The nonlinear distortion is compensated through phase conjugation in the SOA-NLC scheme, and hence, the performance improves with the output power in this case, for all channels. Thus, while comparing the Q^2 values between SOA-NLC and single SOA, the difference in performance decreases with an increase in output power. The region of operation where SOA-NLC outperforms single SOA is shown as a shaded portion in Fig. 4. The average improvement is better than 4 dB for an output power of 4 dBm. Thus, irrespective of expected larger nonlinear distortion from cascaded SOAs operating in the similar operating conditions, sandwiching OPC between them is effective in the nonlinear distortion compensation even with the additional noise figure from the second SOA. Even though the performance difference at higher bias currents is not evaluated, we expect similar trends since the compensation with OPC stage is independent of the gain so long as the bit-pattern effect is avoided.

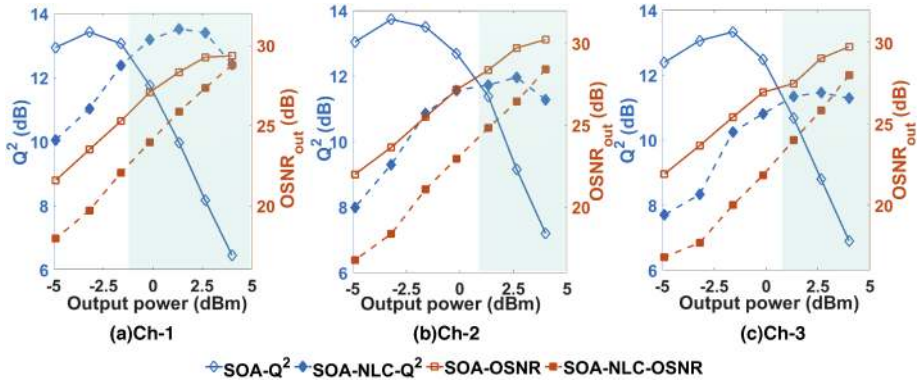

Fig. 4. Q^2 and output OSNR as a function of output power from both SOA and SOA-NLC in back-to-back -3 × 12 Gbaud-16QAM , I_{drive}= 150 mA: (a) Channel 1, (b) Channel 2, (c) Channel 3. The shaded portion indicates the region of operation where SOA-NLC outperforms single SOA

4.3. Transmission through 160 km fiber

The practical advantage of the low distortion higher output power capability of the SOA shown in the B2B result is highlighted in this section by carrying out a transmission of the amplified signal through a long length of the fiber. In a practical implementation, the OSNR at the receiver is dominated by that of the pre-amplifier because of the typically low received powers, and thus the OSNR difference between the output of single SOA and SOA-NLC, discussed in the previous section could not influence the data quality even at low input powers. We verify this claim in the following manner. We find that the received OSNR becomes comparable for both SOA and SOA-NLC output with an approximate attenuation >30 dB. As a practical use case, we transmit the amplified signals from both cases through 160 km long fiber (*attenuation* >30 dB) and compare the Q^2 for a range of input power levels. With this attenuation, the receiver OSNR is found to be comparable (within <1 dB difference) for both the cases, for each value of output power. The results with 16QAM WDM channels for a single SOA and with SOA-NLC are shown in Fig. 5. The receiver OSNR is shown in the right-side y-axis and it is evident that the OSNR difference between the two cases is less than a decibel throughout the range of power levels considered. It is ensured that the power launched in both cases are below the nonlinear threshold of the fiber. The Q^2 value as a function of launch power to the fiber (different output

Optics EXPRESS

power from SOA/SOA-NLC at 150 mA drive current, by varying the SOA input power from -24.5 to -12.5 dBm) for all three channels are shown in Fig. 5.

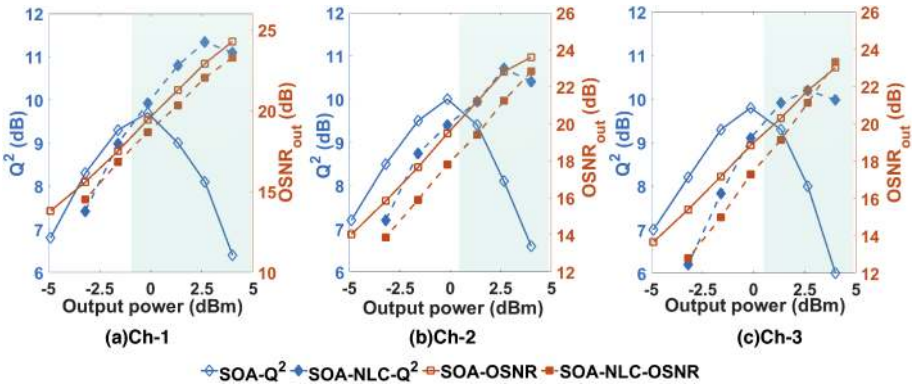

Fig. 5. Q^2 and output OSNR as a function of output power from both SOA and SOA-NLC with 160 km transmission for 3 × 12 Gbaud-16QAM , I_{drive}= 150 mA: (a) Channel 1, (b) Channel 2, (c) Channel 3. The shaded portion indicates the region of operation where SOA-NLC outperforms single SOA

The advantage of the SOA-NLC scheme is evident in the nonlinear regime of operation of the SOA (shaded region in Fig. 5), where the output from single SOA shows a degraded performance. Q^2 improvement is 4.5 dB at the largest power margin (4 dBm launched to the fiber, and received power of ≈ -26 dBm) at a receiver OSNR of ≈ 23 dB. This is enabled primarily because of the larger received powers with lower distortions. In the linear regime, after transmission through 160 km of fiber since the OSNR at the receiver are comparable, the Q^2 performance difference is less than a decibel for SOA and SOA-NLC. It is interesting to note that, in the nonlinear distortion regime, the SOA-NLC configuration not only outperforms the single SOA, the Q^2 value is also found to be larger than that at the best linear operation of single SOA. These results emphasize the capability of the OPC based nonlinear distortion compensation in SOA for higher power margin and long transmission reach.

4.4. Back-to-back operation with 64-QAM

We further prove that SOA-NLC using OPC is an efficient method in reducing the SOA nonlinear phase distortion in higher-order QAM with low phase margin by modulating the WDM signals with 64QAM. For the same power levels, the nonlinear distortion tolerance is smaller for 64QAM modulation compared to 16QAM due to its smaller phase margin [36]. Moreover, the OSNR requirement is higher and hence it is important to study the effect of larger noise figure of SOA-NLC in the distortion compensation for 64QAM modulation. The results in a back-to-back configuration for 3×12 Gbaud 64QAM signal, for the middle channel (Ch2) is shown in Fig. 6. The OSNR variation with the output power is shown in Fig. 6(a) (right y-axis) . Output OSNR is such that the noise figure is more with SOA-NLC compared to that of a single SOA device, as explained before. At lower output power levels, the poorer OSNR poses a limit for SOA-NLC performance and hence, the performance below 0 dBm is not shown with SOA-NLC case. The shaded portion in the figure shows the operating regime where SOA-NLC outperforms the single SOA. Since the nonlinear tolerance is smaller for 64QAM modulated signals, even in the low output power values, the Q^2 performance in the single SOA is moderate. This performance limitation is also due to the poorer OSNR at those power levels compared to the high OSNR requirement for 64QAM. For an output power of > 0 dBm, SOA-NLC outperforms single SOA. At a larger output power of 3 dBm, SOA-NLC achieves approximately 3 dB higher Q^2 factor

Optics EXPRESS

over the single SOA, which generally fails to be demodulated by DSP due to excessive nonlinear distortion. Figure 6(b) shows the BER performance as a function of output power for Channel 2 (Ch2), both for a single SOA device and with SOA-NLC scheme. Constellations corresponding to an output power of 1.5 dBm, are shown for single SOA and that for the SOA-NLC, where larger distortion for the single SOA case is evident. One order of magnitude improvement in BER performance is obtained for the SOA-NLC case. The BER performance is below SD-FEC limit, at power levels larger than >1.5 dBm for the SOA-NLC case, while the demodulation fails for SOA without NLC. Even with poorer OSNR compared to single SOA, the SOA-NLC scheme performs better because of (a) the low-phase margin and hence the lower tolerance to input power variance for nonlinear phase distortion (b) the larger output power with distortion compensation.

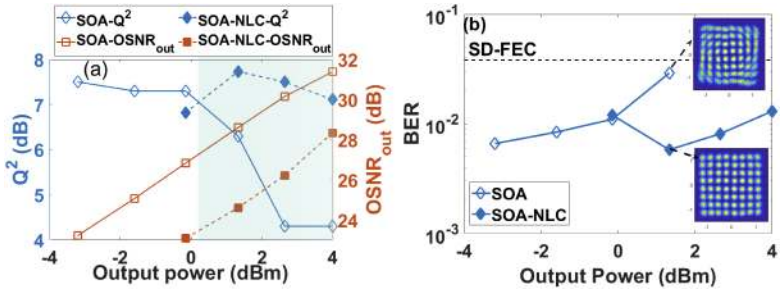

Fig. 6. (a) Q^2 performance and $OSNR_{out}$, (b) BER performance, as a function of output power for back-to-back- 3 × 12 Gbaud-64QAM, Ch-2: The shaded portion indicates the region of operation where SOA-NLC outperforms single SOA. The SD-FEC is marked as a dashed line (BER= 3.8×10^{-2}).

5. Discussion

We have presented the detailed experimental results to prove that the nonlinear distortions from an SOA can be significantly suppressed when two similar SOAs are used with an OPC stage sandwiched between them. The operating condition for this SOA-NLC scheme should be such that the two SOAs should operate in a similar nonlinear regime. Since our experiments use two discrete SOAs, we carried out a detailed characterization to identify the operating point. A practically feasible way forward would be to use two SOAs, fabricated in the same substrate under similar conditions to ensure the same structural and functional properties. This will enable Henry's linewidth enhancement factor of the two SOAs to be similar and the symmetric and wavelength-independent operation will be possible with much more flexibility. We would also like to reiterate that the proposed scheme is expected to enable such large nonlinear distortion compensation only in the absence of the bit-pattern effect. Whenever the gain-recovery of the SOA is longer than the time scales at which the symbol changes, the consequent amplitude distortions cannot be compensated by the proposed OPC scheme. In the presence of bit-pattern effects, the envelope of the signal at the input and output of the first SOA will be different, which will make it difficult to carry out a distortion cancellation in the second SOA stage after the OPC. However, even for such a slower gain response case, if the pattern effects are well suppressed by some other means while entailing nonlinear phase distortions, the OPC based SOA NLC could be still effective. Investigation of its effective range for the slow SOAs would be a subject of future investigation. While a high-performance broadband OPC set-up was implemented with HNLF for this proof of principle experiment investigating the efficacy of OPC for compensating nonlinear distortion in SOAs, which could potentially be replaced with SOA [23]. All-SOA solution for compensating nonlinear distortion, could reduce the power consumption and allow flexible on-chip integration with a smaller footprint.

Optics EXPRESS

6. Conclusion

In summary, we have proved experimentally that the nonlinear distortions from an SOA can be significantly suppressed when two SOAs are used with an OPC stage sandwiched between them. Irrespective of the larger ASE noise from two cascaded SOAs, the OPC was proved to be capable of reducing nonlinear distortions from the SOAs even overcoming the additional ASE noise. The attenuation associated with the OPC and the additional SOA intrinsically worsen the ASE noise figure of this scheme. However, this was mostly inconsequential for 160km transmission. Here, we should note that symbol-period, longer than the gain recovery time of the SOAs was chosen to suppress the bit-pattern effects. Thus, the scheme is expected to perform at its best for any system with a symbol-rate smaller than the inverse of the gain recovery time of the SOAs under consideration. The efficacy of the scheme for higher order modulation format (> 64QAM) need to be studied in future. In the 16QAM back-to-back configuration, although the single SOA case outperforms the OPC-NLC case in the low power region due to (a) the larger OSNR difference between the two and (b) low distortions, superiority reverses at a larger output power where the nonlinear distortion per SOA grows with increasing OSNR. In fact, the average Q^2 improvement more than 4 dB was observed for an output power of 4 dBm. With comparable receiver OSNR with 160 km fiber transmission, Q^2 performance at a larger output power of SOA-NLC was better than that of single SOA even at its low power linear operating regime. With higher-order QAM (64QAM) having low-phase margin and low nonlinear phase noise tolerance, SOA-NLC outperformed single SOA in a back-to-back configuration with an improved Q^2 value by 3 dB at an output power of 3 dBm. These results show the capability of optical phase conjugation enabling large output power with low-distortion from semiconductor optical amplifiers in low WDM channel count applications.

A. Appendix

The SOA-NLC scheme works most effectively when the two SOAs have symmetric performances in terms of wavelength, gain and nonlinearity as discussed in Section 2. We present the details of identifying the operating regimes- in terms of wavelengths and gain values. These experiments are carried out with QPSK modulation of symbol-rate 12 Gbaud with a PRBS $2^{15} - 1$ pattern. QPSK modulation is chosen so that its larger phase margin allows a larger input power dynamic range for the nonlinear characterization. Though the characterization is shown for a drive current of 250 mA, the symmetric properties of two SOAs are not expected to be drastically different at different drive currents.

We first quantify the gain as a function of input power for all three channels in both SOAs. Across all the three channels, the gain reduces with increase in total input power for both the SOAs. The slope of the gain saturation curves (Fig. 7(a) & (b)) are similar for both the SOAs and for all the three channels, but the 3-dB saturation powers are found to be slightly different. To identify the optimal choice of WDM wavelength for the proof of concept demonstration, we measure the performance of the amplified signal in terms of Q^2 at the output of the SOA for an input power of -12 dBm and drive current of 250 mA. The frequency of all the three WDM channels is tuned in this experiment while maintaining the channel separation to be 50 GHz (the middle WDM channel (CH2) at the center frequency is shown here for the reference). As evident in Fig. 7(a) & (b), this input power level is high enough to make the operating conditions nonlinear. Figure 7(c) shows the Q^2 measured for all the three channels for both the SOAs, under the same operating condition (input power of -12 dBm drive current of 250 mA), but operated independently. Frequency of all the three WDM channels is tuned (CH2 is shown here) while maintaining the WDM channel spacing. SOA1- is found to be more resilient to wavelength change in terms of the Q^2 performance. The output channel flatness and hence the channel performance in SOA2 is found to be wavelength-dependent. On further investigation, we found

Optics EXPRESS

that this specific SOA has a significantly larger gain ripple in its ASE spectrum (not shown here), possibly due to higher reflections from end facets, leading to wavelength dependent channel performance. The Q^2 performance is also found to progressively decrease with increase in the center frequency in both the SOAs (as shown in Fig. 7(c)) due to the nature of the gain spectrum. Hence, the lowest frequency which provides larger Q^2 and similar performance across the three channels need to be identified. This condition is satisfied at the frequency 192.65 THz and is chosen as the center frequency of the WDM system. The optical phase conjugate frequencies are designed such that those are in the nearest frequencies as that of the signal and that the Q^2 factor difference between the signal and the conjugate is minimal. Thus the center frequency of conjugates is chosen at 193.05 THz where the performance deviation across the channels for one of the two SOAs is minimum. These frequencies are marked with dotted circles in the Fig. 7(c). The pump frequencies in the OPC stage are chosen to achieve this conjugate frequency, for the chosen signal frequency. The residual differences in the channels flatness at the output of the SOAs even at the optimal wavelengths chosen could lead to differences in performances in these channels. SOA1 is more flexible in terms of wavelength dependence (Ref. Figure 7 (c). Thus the SOA1 is chosen to be the device after the OPC stage where the design flexibility in terms of the input parameters is limited. The overall loss of the OPC stage is adjusted so that the input power to the two SOA stages are the same. Note that, this process of optimal choice is very elaborate only because we used two independent commercial SOAs for this proof-of-principle experiment. In a practical implementation, when the two SOAs are grown on the same substrate and similarly processed, this characterization could be much simpler.

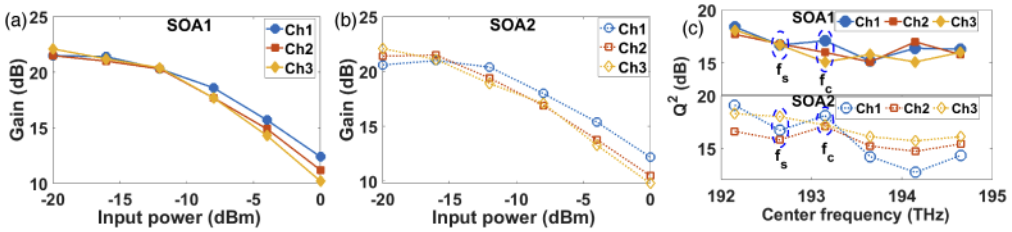

Fig. 7. SOA characterization at I_{drive}= 250 mA with 3× 12 Gbaud QPSK: Gain as a function of input power for (a) SOA1 and (b) SOA2, (c) Q^2 of three channels across the C-band wavelength for two SOAs. The signal frequency (192.65 THz) and the conjugate frequency (193.05 THz) used for the experiments are marked in dotted circles.

B. Appendix

The Q factor is calculated from the waveform assuming that the distribution at each amplitude level is a simple Gaussian function. The Q-factor of a k-level PAM signal is defined as follows,

$$Q = \frac{1}{k-1} \sum_{i=1}^{i=k-1} \frac{|\mu_i - \mu_{i+1}|}{\sigma_i + \sigma_{i+1}}, \tag{6}$$

where, the μ_i is the mean and σ_i is the variance of the Gaussian function at i^{th} amplitude level. For m-QAM signals, the Q-factor is calculated for both in-phase (Q_R) and quadrature (Q_I) waveform. Further the net Q is calculated as $Q = \sqrt{Q_I^2 + Q_R^2}$, and then Q^2 in dB is Q^2 [dB]= $20\log_{10}(Q)$.

Optics EXPRESS

C. Appendix

The theoretical BER is calculated as [35]:

$$BER = \frac{2}{\log_2(M)}\left(1 - \frac{1}{\sqrt{M}}\right)\text{erfc}\left(\sqrt{\frac{3 \times SNR}{2(M-1)}}\right) \tag{7}$$

where, $M = 16$ for 16QAM and $M = 64$ for 64QAM signals, SNR represents the electrical SNR related to OSNR as [34]:

$$SNR = \frac{2 \times B_{ref} \times OSNR}{p \times R_s}. \tag{8}$$

B_{ref}- the reference bandwidth in GHz for OSNR calculation (12.5 GHz), R_s- symbol-rate of the signal, $p = 1$ for single polarization and OSNR of the signal expressed in the linear scale.

Now, Q can be theoretically estimated from $BER - Q$ relation as [34]:

$$BER = \frac{1}{2}\text{erfc}\left(\frac{Q}{\sqrt{2}}\right) \tag{9}$$

Q^2 is calculated from Eq. (9) and converted to logarithmic scale.

Funding. Department of Science and Technology, Ministry of Science and Technology, India; Ministry of Electronics and Information technology (MEITY-PHD-2695, Visvesvaraya PhD Scheme); Ministry of Human Resource Development (SPARC).

Disclosures. The authors declare no conflicts of interest.

References

1. J. Renaudier and A. Ghazisaeidi, "Scaling capacity growth of fiber-optic transmission systems using 100+nm ultra-wideband semiconductor optical amplifiers," J. Lightwave Technol. **37**(8), 1831–1838 (2019).
2. J. Xu, X. Zhang, and J. Moerk, "Investigation of patterning effects in ultrafast SOA-based optical switches," IEEE J. Quantum Electron. **46**(1), 87–94 (2010).
3. M. Amaya and A. Sharaiha, "Crosstalk pattern penalty reduction at 2.5Gb/s in an SOA employing an assist light around gain transparency wavelength," Opt. Commun. **261**(2), 240–244 (2006).
4. E. A. Patent, J. J. G. M. van der Tol, Y. S. Oei, M. K. Smit, M. L. Nielsen, J. Mork, and J. J. M. Binsma, "Integrated SOA-MZI for pattern-effect-free amplification," Electron. Lett. **41**(9), 549–551 (2005).
5. T. Akiyama, N. Hatori, Y. Nakata, H. Ebe, and M. Sugawara, "Pattern-effect-free semiconductor optical amplifier achieved using quantum dots," Electron. Lett. **38**(19), 1139–1140 (2002).
6. D. F. Bendimerad and Y. Frignac, "Numerical investigation of SOA nonlinear impairments for coherent transmission systems based on SOA amplification," J. Lightwave Technol. **35**(24), 5286–5295 (2017).
7. W. Hong, M. Li, X. Zhang, J. Sun, and D. Huang, "Noise Suppression Mechanisms in Regenerators Based on XGC in an SOA With Subsequent Optical Filtering," IEEE J. Sel. Top. Quantum Electron. **18**(2), 935–949 (2012).
8. A. Bhardwaj, C. R. Doerr, S. Chandrasekhar, and L. W. Stulz, "Reduction of nonlinear distortion from a semiconductor optical amplifier using an optical equalizer," IEEE Photonics Technol. Lett. **16**(3), 921–923 (2004).
9. C. Tai, S. L. Tzeng, H. C. Chan, and W. I. Way, "Reduction of nonlinear distortion in MQW semiconductor optical amplifier using light injection and its application in multichannel M-QAM signal transmission systems," IEEE Photonics Technol. Lett. **10**(4), 609–611 (1998).
10. H. H. Lu, W. J. Wang, H. S. Su, and C. T Wang, "Reduction of semiconductor optical amplifier induced distortion and crosstalk in a 1.3-μm WDM transport system," IEEE Photonics Technol. Lett. **15**(5), 775–777 (2003).
11. M. M. Resende, P. Tovar, G. C. Amaral, and J. P. von der Weid, "Overcoming the maximum amplification limit of coherent optical pulses in semiconductor optical amplifiers with time-polarization multiplexing," Opt. Eng. **56**(11), 1 (2017).
12. F. Hamaoka, S. Okamoto, M. Nakamura, A. Matsushita, and Y. Kisaka, "Adaptive compensation for SOA-induced nonlinear distortion with training-based estimation of SOA device parameters," **pp. 1-3**, ECOC (2018).
13. A. Ghazisaeidi and L. A. Rusch, "On the efficiency of digital back-propagation for mitigating SOA-induced nonlinear impairments," J. Lightwave Technol. **29**(21), 3331–3339 (2011).
14. F. Vacondio, A. Ghazisaeidi, A. Bononi, and L. A. Rusch, "Low-complexity compensation of SOA nonlinearity for single-channel PSK and OOK," J. Lightwave Technol. **28**(3), 277–288 (2010).
15. Y. Lin, E. Giacoumidis, S. O'Duill, and L. P. Barry, "DBSCAN-based clustering for nonlinearity induced penalty reduction in wavelength conversion systems," IEEE Photonics Technol. Lett. **31**(21), 1709–1712 (2019).

Optics EXPRESS

16. A. Arnould, A. Ghazisaeidi, D. Le Gac, P. Brindel, M. Makhsiyan, K. Mekhazni, F. Blache, M. Achouche, and J. Renaudier, "Experimental characterization of nonlinear distortions of semiconductor optical amplifiers in the WDM regime," J. Lightwave Technol. **38**(2), 509–513 (2020).
17. A. A. I. Ali, M. Al-Khateeb, T. Zhang, F. Ferreira, and A. Ellis, "Enhanced nonlinearity compensation efficiency of optical phase conjugation system," **paper. Th2A.11**, OFC (2019).
18. K. Solis-Trapala, M. Pelusi, H. Nguyen Tan, T. Inoue, and S. Namiki, "Optimized WDM transmission impairment mitigation by multiple phase conjugations," J. Lightwave Technol. **34**(2), 431–440 (2016).
19. K. R. H. Bottrill, N. Taengnoi, F. Parmigiani, D. J. Richardson, and P. Petropoulos, "PAM4 transmission over 360 km of fibre using optical phase conjugation," OSA Continuum **2**(3), 973–982 (2019).
20. S. Yoshima, Y. Sun, Z. Liu, K. R. H. Bottrill, F. Parmigiani, D. J. Richardson, and P. Petropoulos, "Mitigation of Nonlinear Effects on WDM QAM Signals Enabled by Optical Phase Conjugation With Efficient Bandwidth Utilization," J. Lightwave Technol. **35**(4), 971–978 (2017).
21. T. Umeki, T. Kazama, A. Sano, K. Shibahara, K. Suzuki, M. Abe, H. Takenouchi, and Y. Miyamoto, "Simultaneous nonlinearity mitigation in 92 × 180-Gbit/s PDM-16QAM transmission over 3840 km using PPLN-based guard-band-less optical phase conjugation," Opt. Express **24**(15), 16945–16951 (2016).
22. F. Da Ros, A. Gajda, E. P. da Silva, A. Peczek, A. Mai, K. Petermann, L. Zimmermann, L. Katsuo Oxenlowe, and M. Galili, "Optical phase conjugation in a silicon waveguide With lateral p-i-n diode for nonlinearity compensation," J. Lightwave Technol. **37**(2), 323–329 (2019).
23. A. Sobhanan, V. A. M. Karthik, L. V. Narayanan, R. D. Koilpillai, and D. Venkitesh, "Experimental analysis of noise transfer in optical phase conjugation process in nonlinear SOA," **paper. W2A.38**, OFC (2019).
24. A. Sobhanan, L. N. Venkatasubramani, R. D. Koilpillai, and D. Venkitesh, "Dispersion and Nonlinearity Distortion Compensation of the QPSK/16QAM Signals Using Optical Phase Conjugation in Nonlinear SOAs," IEEE Photonics J. **12**(1), 1–7 (2020).
25. A. Sobhanan, M. Pelusi, T. Inoue, D. Venkitesh, and S. Namiki, "Compensation of SOA Nonlinear Distortions by Mid-stage Optical Phase Conjugation," **paper M1I.5**, OFC (2020).
26. M. Sugawara, H. Ebe, N. Hatori, M. Ishida, Y. Arakawa, T. Akiyama, K. Otsubo, and Y. Nakata, "Theory of optical signal amplification and processing by quantum-dot semiconductor optical amplifiers," Phys. Rev. B **69**(23), 235332 (2004).
27. W. Mathlouthi, F. Vacondio, P. Lemieux, and L. A. Rusch, "SOA gain recovery wavelength dependence: simulation and measurement using a single-color pump-probe technique," Opt. Express **16**(25), 20656–20665 (2008).
28. H. J. S. Dorren, D. Lenstra, Y. Liu, M. T. Hill, and G. D. Khoe, "Nonlinear polarization rotation in semiconductor optical amplifiers: theory and application to all-optical flip-flop memories," IEEE J. Quantum Electron. **39**(1), 141–148 (2003).
29. A. Marculescu, S. Ó. Dúill, C. Koos, W. Freude, and J. Leuthold, "Spectral signature of nonlinear effects in semiconductor optical amplifiers," Opt. Express **25**(24), 29526–29559 (2017).
30. P. M. Kaminski, F. Da Ros, E. P. da Silva, M. Pu, M. P. Yankov, E. Semenova, K. Yvind, A. T. Clausen, S. Forchhammer, L. K. Oxenlowe, and M. Galili, "Characterization and Optimization of Four-Wave-Mixing Wavelength Conversion System," J. Lightwave Technol. **37**(21), 5628–5636 (2019).
31. H. Hu, R. Nouroozi, R. Ludwig, C. S. Langhorst, H. Suche, W. Sohler, and C. Schubert, "110 km transmission of 160 Gbit/s RZ-DQPSK signals by midspan polarization-insensitive optical phase conjugation in a Ti:PPLN waveguide," Opt. Lett. **35**(17), 2867–2869 (2010).
32. T. Umeki, T. Kobayashi, A. Sano, T. Ikuta, M. Abe, T. Kazama, K. Enbutsu, R. Kasahara, and Y. Miyamoto, "Nonlinearity mitigation of PDM-16QAM signals using multiple CSI-OPCs in ultra-long-haul transmission without excess penalty," IEICE Trans. Commun. **E103.B**(11), 1226–1232 (2020).
33. S. Watanabe, S. Takeda, and T. Chikama, "Interband wavelength conversion of 320 Gb/s (32/spl times/10 Gb/s) WDM signal using a polarization-insensitive fiber four-wave mixer," **3**, pp. 83–87, ECOC(1998).
34. G. P. Agrawal, *Fiber-optic communication systems*, 3rd ed., (John Wiley & Sons, Inc., 2002).
35. R. A. Shafik, M. S. Rahman, and A. H. M. R. Islam, "On the extended relationships among EVM BER and SNR as performance metrics," *Proc. 4th Int. Conf. Electrical and Computer Engineering (ICECE 2006)*, pp. 408–411 (2006).
36. M. Paskov, "Algorithms and Subsystems for Next Generation Optical Networks," Doctoral Thesis, **UCL** (2015).